Neuron
Article

Interplay between Cytosolic Dopamine, Calcium, and α-Synuclein Causes Selective Death of Substantia Nigra Neurons

Eugene V. Mosharov,[1] Kristin E. Larsen,[1] Ellen Kanter,[1] Kester A. Phillips,[1] Krystal Wilson,[1] Yvonne Schmitz,[1] David E. Krantz,[2] Kazuto Kobayashi,[3] Robert H. Edwards,[4] and David Sulzer[1,5,6,*]
[1]Department of Neurology, Columbia University Medical Center, New York, NY 10032, USA
[2]Department of Psychiatry and Biobehavioral Sciences, The David Geffen School of Medicine, University of California, Los Angeles, Los Angeles, CA 90095, USA
[3]Department of Molecular Genetics, Fukushima Medical University School of Medicine, 1 Hikarigaoka, Fukushima 960-1295, Japan
[4]Departments of Neurology and Physiology, University of California School of Medicine, San Francisco, CA 94143, USA
[5]Department of Psychiatry and Pharmacology, Columbia University Medical Center, New York, NY 10032, USA
[6]Division of Molecular Therapeutics, New York Psychiatric Institute, New York, NY 10032, USA
*Correspondence: ds43@columbia.edu
DOI 10.1016/j.neuron.2009.01.033

SUMMARY

The basis for selective death of specific neuronal populations in neurodegenerative diseases remains unclear. Parkinson's disease (PD) is a synucleinopathy characterized by a preferential loss of dopaminergic neurons in the substantia nigra (SN), whereas neurons of the ventral tegmental area (VTA) are spared. Using intracellular patch electrochemistry to directly measure cytosolic dopamine (DA_{cyt}) in cultured midbrain neurons, we confirm that elevated DA_{cyt} and its metabolites are neurotoxic and that genetic and pharmacological interventions that decrease DA_{cyt} provide neuroprotection. L-DOPA increased DA_{cyt} in SN neurons to levels 2- to 3-fold higher than in VTA neurons, a response dependent on dihydropyridine-sensitive Ca^{2+} channels, resulting in greater susceptibility of SN neurons to L-DOPA-induced neurotoxicity. DA_{cyt} was not altered by α-synuclein deletion, although dopaminergic neurons lacking α-synuclein were resistant to L-DOPA-induced cell death. Thus, an interaction between Ca^{2+}, DA_{cyt}, and α-synuclein may underlie the susceptibility of SN neurons in PD, suggesting multiple therapeutic targets.

INTRODUCTION

Parkinson's disease (PD) is characterized by aggregation of alpha-synuclein (α-syn) into Lewy bodies and Lewy neurites, and a progressive loss of specific neuronal populations. In particular, ventral midbrain (VM) dopamine (DA) neurons of the substantia nigra (SN) preferentially degenerate in PD, while neighboring ventral tegmental area (VTA) DA neurons are relatively spared (Dauer and Przedborski, 2003). A role of α-syn in PD pathogenesis is demonstrated by cases of familial PD that result from mutations or overexpression of α-syn, as well as by the observation that SN neurons in mice with α-syn deletion are protected against the parkinsonian neurotoxins MPTP and 6-OHDA (Alvarez-Fischer et al., 2008; Dauer et al., 2002). Several hypotheses may explain α-syn-mediated cytotoxicity, including the formation of toxic aggregates that disrupt membrane (Conway et al., 2001), a blockade of lysosomal protein degradation (Martinez-Vicente et al., 2008), and mitochondrial dysfunction (Ved et al., 2005). It has also been recently suggested that high Ca^{2+} levels due to $Ca_v1.3$ channel-dependent pacemaking activity (Nedergaard et al., 1993) may contribute to SN susceptibility, as VTA neurons use Na^+ channels for pacemaking (Chan et al., 2007). Accordingly, $Ca_v1.3$ antagonists block SN cell death in MPTP and other neurotoxin models (Chan et al., 2007). The reason for the preferential death of SN DA neurons is, however, unclear, as both α-syn and $Ca_v1.3$ channels are expressed throughout the CNS in neurons that are not lost in PD (Clayton and George, 1998; Rajadhyaksha et al., 2004; Striessnig et al., 2006).

A long-standing hypothesis of neurodegeneration in PD postulates that the buildup of cytosolic DA (DA_{cyt}) with associated oxyradical stress and its possible interaction with α-syn and other PD-related proteins underlie neurotoxicity (Caudle et al., 2008; Chen et al., 2008; Edwards, 1993; Pardo et al., 1995; Sulzer and Zecca, 2000). A role for DA_{cyt} in the selectivity of cell death in PD, however, has never been directly studied due to a lack of means to measure DA_{cyt}. Here we use a new electrochemical approach to measure DA_{cyt} in neurons following various pharmacological and genetic interventions. We report that "multiple hits" consisting of high cytoplasmic Ca^{2+}, elevated DA_{cyt}, and α-syn expression are required to evoke selective death of dopaminergic neurons from SN and show that interference with any of these three factors rescues the neurons.

RESULTS

We previously introduced intracellular patch electrochemistry (IPE) to study the regulation of cytosolic catecholamine

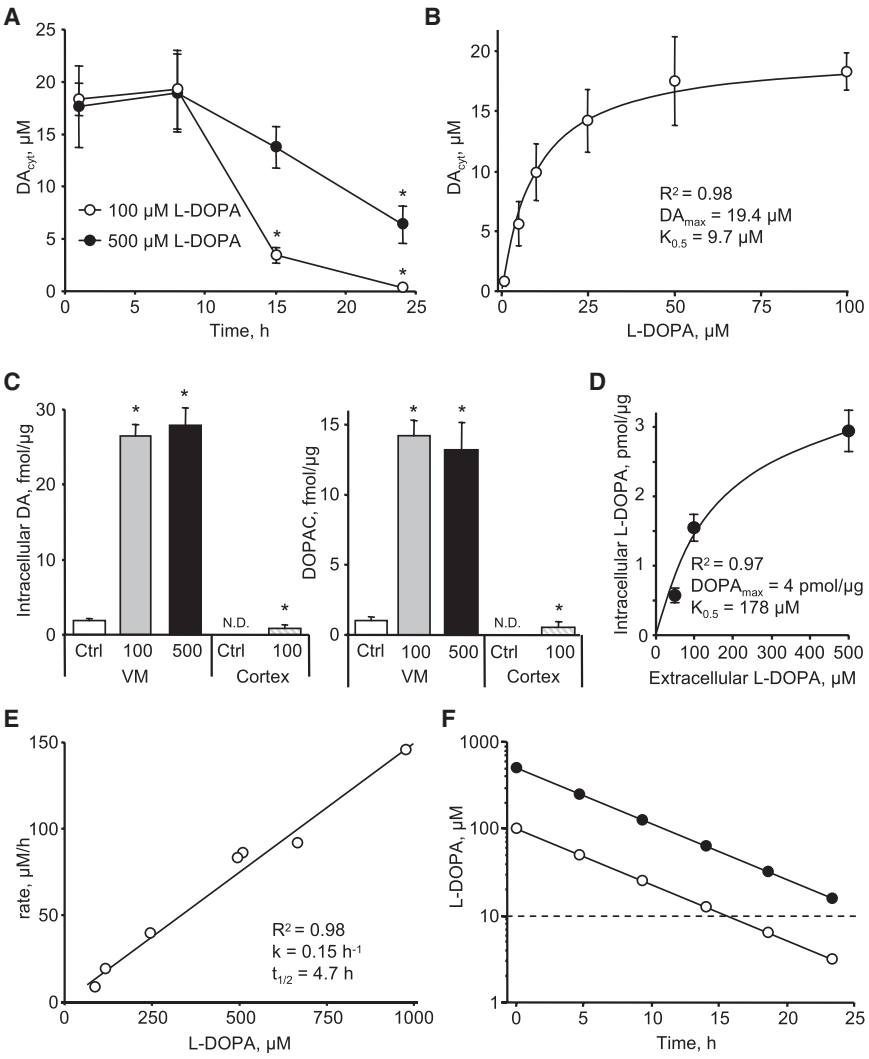

Figure 1. L-DOPA Metabolic Consumption by VM Neurons

(A) Time dependence of DA_{cyt} following cell treatment with two L-DOPA concentrations. *$p < 0.05$ versus 1 hr time point by one-way ANOVA (n = 9–52 cells in different groups).

(B) Dependence of DA_{cyt} on extracellular L-DOPA in mouse neurons treated with the drug for 1 hr (n = 10–24 cells). Solid line indicates the fit of the data points using the equation $[DA_{cyt}] = DA_{max}*[L\text{-}DOPA]/(K_{0.5} + [L\text{-}DOPA])$.

(C) HPLC-EC measurements of the total intracellular DA and DOPAC in rat VM (n = 9 dishes) and cortical (n = 3) neuronal cultures exposed to 100 or 500 μM L-DOPA for 1 hr; N.D., not detected. *$p < 0.05$ versus untreated cultures.

(D) HPLC measurements of intracellular L-DOPA contents in rat VM cultures pretreated with the AADC inhibitor benserazide (2 μM; 1 hr) and then treated with 50, 100, or 500 μM L-DOPA for 1 hr (n = 3–8 dishes). Solid line indicates the fit of the data points using the equation $[L\text{-}DOPA_{intracell}] = DOPA_{max}*[L\text{-}DOPA_{extracell}]/(K_{0.5} + [L\text{-}DOPA_{extracell}])$.

(E) Dependence of the rate of L-DOPA auto-oxidation on the initial L-DOPA concentration determined by HPLC-EC in a cell-free system. The half-life was calculated from the incline (k) of the linear fit of the data points as $t_{1/2} = Ln(2)/k$.

(F) Time dependence of extracellular L-DOPA concentration modeled using kinetic constants from (E). The dashed line indicates $K_{0.5}$ from (B). Data in (A)–(D) are means ± SEM.

homeostasis in cultured primary murine adrenal chromaffin cells (Mosharov et al., 2003) and the PC12 cell line (Mosharov et al., 2006). To extend IPE measurements to DA neurons, we employed VM cultures from mice that express green fluorescent protein under the control of the tyrosine hydroxylase (TH) promoter (TH-GFP; see Figure S1 available online) (Sawamoto et al., 2001). Immunolabeling of fixed 2-week-old cultures of VM neurons for TH showed that approximately 97% of GFP^+ cells were TH^+ (185 of 191 cells).

Dependence of DA_{cyt} on Extracellular L-DOPA

IPE measurements in cyclic voltammetric (CV) mode that detects DA preferentially over other intracellular metabolites (including L-3,4-dihydroxyphenylalanine [L-DOPA] and dihydroxyphenylacetic acid [DOPAC]) revealed that DA_{cyt} in untreated GFP^+ neurons was below the detection limits of the technique (<0.1 μM). This was similar to DA_{cyt} levels in PC12 cells (Mosharov et al., 2006), but differed from the 10–20 μM cytosolic catecholamine concentrations found in untreated chromaffin cells (Mosharov et al., 2003). We previously demonstrated that 1 hr pretreatment with 100 μM L-DOPA produces a 2- to 3-fold increase of cytosolic catecholamine concentration in chromaffin cells (Mosharov et al., 2003). The same dose of L-DOPA increased DA_{cyt} in GFP^+ neurons to 17.4 ± 1.7 μM (mean ± SEM; n = 74 cells).

To determine the kinetics of DA_{cyt} changes after L-DOPA treatment, we performed IPE at 1, 8, 15, and 24 hr after L-DOPA addition to the media. After 1 hr of 100 μM L-DOPA exposure, DA in the cytosol reached a steady-state level that was maintained for ~8 hr, followed by a decline to control levels over the succeeding 24 hr of drug treatment (Figure 1A). Interestingly, 500 μM L-DOPA increased DA_{cyt} to the same maximum level, but the elevated steady state was maintained longer, and 24 hr after L-DOPA treatment, DA_{cyt} was still higher than in untreated cells. To study the dependence of DA_{cyt} on extracellular L-DOPA, neuronal cultures were treated with a range of L-DOPA concentrations for 1 hr at 37°C, followed by IPE measurements in the presence of the same L-DOPA concentrations in the bath and in the pipette solutions within the following 30 min at room temperature. The drug response curve was hyperbolic (Figure 1B) with an apparent $K_{0.5}$ of ~10 μM L-DOPA.

As the steady-state DA concentration in neuronal cytosol is regulated by multiple enzymes and transporters, we attempted to determine which metabolic step limited DA_{cyt} accumulation in L-DOPA-treated cells. High-performance liquid chromatography

with electrochemical detection (HPLC-EC) measurements of the total intracellular DA (the majority of which represents vesicular DA; Chien et al., 1990; Mosharov et al., 2003) and DOPAC contents showed that these metabolites were elevated to the same degree in neurons exposed to 100 and 500 μM L-DOPA (Figure 1C), indicating that there was no difference in the rates of DA oxidation by monoamine oxidase A (MAO) and vesicular uptake by vesicular monoamine transporter 2 (VMAT2). To establish whether L-DOPA transport into the cell or its conversion to DA by aromatic L-amino acid decarboxylase (AADC) limited the L-DOPA metabolic consumption, we measured total intracellular L-DOPA levels in VM cultures after 1 hr treatment with 100 and 500 μM L-DOPA concentrations in the presence of the AADC inhibitor benserazide to block DA synthesis (Figure 1D). The initial rate of L-DOPA accumulation in the cells was not saturated under these conditions, consistent with previously published data (Sampaio-Maia et al., 2001) on the kinetics of L-DOPA uptake by cell lines derived from astrocytes and neurons (K_m = 50–100 μM). Overall, these data suggest that the activity of AADC limits the steady-state DA_{cyt} concentration following L-DOPA treatment.

The data in Figure 1C also provide information about the rate of L-DOPA turnover by the cells. The combined rate of DA and DOPAC synthesis during 1 hr of L-DOPA exposure was ~40 fmol/μg of total protein. As each culture dish typically contained 50 −100 μg of total protein, the rate of L-DOPA consumption during 10 hr of incubation was 20–40 pmol per culture. This rate, however, is too low to account for the decline in the DA_{cyt} observed after 10 hr of cell incubation with L-DOPA (Figure 1A), as the total amount of available L-DOPA was >3 orders of magnitude higher (200 nmol in 2 ml of 100 μM solution). We therefore examined the availability of extracellular L-DOPA, which is known to auto-oxidize to DOPA-semiquinone and DOPA-quinone derivatives (Sulzer and Zecca, 2000). HPLC-EC measurements of L-DOPA concentration in cell-free media showed that the drug disappeared with first-order kinetics and a half-life of 4.7 hr (Figure 1E). This suggests that after 100 or 500 μM L-DOPA initial doses, its concentration in the media would reach the $K_{0.5}$ levels in 16 or 26 hr, respectively (Figure 1F), which is in close agreement with the kinetics of DA_{cyt} changes, as a significant decrease in its initial steady state was observed at approximately these time points (Figure 1A). Together, these data allow us to predict the time dependence of DA_{cyt} changes based on the concentration of L-DOPA added to the media and the initial increase in DA_{cyt} determined by IPE (see Discussion).

L-DOPA-Induced Neurotoxicity

We next investigated whether exposure to various L-DOPA concentrations, and thereby different durations of sustained elevated DA_{cyt}, correlated with neurotoxicity. We identified an exponential dependence of neurotoxicity on the extracellular L-DOPA concentration (Figure 2A), whereas the time dependence for cell survival in cultures treated with 250 μM L-DOPA demonstrated that the number of TH^+ neurons declined linearly after drug exposure, reaching ~50% of the control levels after 4 days, with no subsequent neuronal loss (Figure 2B). As L-DOPA at this concentration is cleared within ~22 hr, the data indicate a lag between the end of L-DOPA/DA-mediated stress and the completed course of the catechol-induced toxicity. For

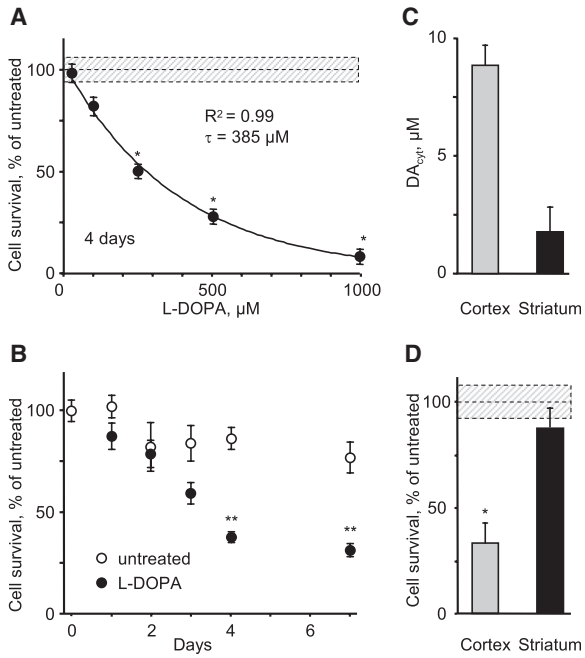

Figure 2. L-DOPA-Induced Neurotoxicity in DA and Non-DA Neurons

(A) The loss of TH^+ neurons in mouse VM cultures treated with different L-DOPA concentrations for 4 days. A similar decline in the number of VMAT2-positive neurons was observed (data not shown). The average number and the density of TH^+ neurons in untreated cultures were 200–250 neurons/culture and 10–15 neurons/mm^2, respectively. The solid line is the fit of the data with an exponential decay function. *p < 0.001 versus age-matched controls by one-way ANOVA.

(B) Time dependence of DA neuron survival in cultures treated with 250 μM L-DOPA. **p < 0.001 versus untreated cells by two-way ANOVA (n = 3–4 dishes).

(C) DA_{cyt} in mouse cortical (n = 59) and striatal (n = 21) neurons incubated with 100 μM L-DOPA for 1 hr.

(D) L-DOPA-induced toxicity in cortical and striatal neurons exposed to 250 μM for 4 days and immunostained for MAP2. *p < 0.01 versus untreated cells by t test (n = 3–5 dishes).

Dotted lines and shadowed boxes in (A) and (D) represent mean ± SEM in untreated cells.

further experiments we exposed cultures to 250 μM L-DOPA, which consistently produced ~50% loss of VM dopaminergic neurons 4 days following drug addition.

Extracellular DA released by neuronal activity did not seem to play a significant role in the L-DOPA-induced cell death, as neuronal viability was not affected by the Na^+ channel blocker tetrodotoxin (TTX; 1 μM), which inhibits stimulation-dependent transmitter release (data not shown). To further determine which pool of DA was responsible for the observed cell damage, we employed postnatal cultures of cortical and striatal neurons, which do not express TH, DAT, or VMAT. Following L-DOPA treatment of cortical neurons, we detected small amounts of DA measured by HPLC-EC (Figure 1C) and a substantial elevation of DA_{cyt} measured by IPE (Figure 2C). This was accompanied by >60% loss of cells immunoreactive to microtubule-associated protein 2 (MAP2), which was used as a neuronal marker (Figure 2D). L-DOPA neurotoxicity was NSD-1015 sensitive,

confirming AADC-mediated DA synthesis in cortical neurons (data not shown). In contrast, almost no DA_{cyt} was detected in L-DOPA-treated striatal neurons, and they were spared following L-DOPA challenge (Figures 2C and 2D). Together, our data suggest DA_{cyt} as the primary source of the L-DOPA-induced neurotoxicity.

Pharmacological Manipulation of DA_{cyt} and Neurotoxicity

AADC, MAO, and VMAT Inhibitors

To study the contribution of individual metabolic pathways in the maintenance of the DA_{cyt} steady state and to determine whether changes in DA level correlate with neurotoxicity, we performed metabolite measurements and toxicity studies on L-DOPA-treated neurons that were preincubated with specific inhibitors of AADC, MAO, and VMAT. Inhibition of the DA-synthesizing enzyme AADC with NSD-1015 (Figures 3A and 3B) or benserazide (not shown) blocked L-DOPA-induced elevation of whole-cell intracellular DA and DOPAC. Benserazide also inhibited the buildup of DA_{cyt} following L-DOPA treatment (Figure 3C), consistent with the idea that the IPE oxidation signal comes from DA synthesized by AADC in the cytosol (note that NSD-1015 alters IPE sensitivity for DA, and therefore was not examined; see Experimental Procedures). Moreover, the blockade of L-DOPA decarboxylation completely prevented drug-induced cell death (Figure 3D), indicating that an L-DOPA metabolite, but not L-DOPA itself, was responsible for the toxicity.

The contribution of DA catabolism was investigated by treating cells with pargyline, an inhibitor of MAO that almost completely abolished DOPAC synthesis (Figure 3B). Pargyline also produced a several-fold increase in both the total amount of intracellular DA (Figure 3A) and DA_{cyt} (Figure 3C) in L-DOPA-treated neurons, which further correlated with a significantly greater neuronal loss (Figure 3D).

The blockade of VMAT-mediated DA uptake into the vesicles depletes vesicular catecholamine storage, as observed by a reduction in the exocytotic quantal size (Colliver et al., 2000). Consistently, pretreatment of VM neurons with reserpine decreased the amount of total intracellular DA synthesized from L-DOPA by ~2-fold both with and without pargyline (Figure 3A). We observed, however, no effect of reserpine, or another VMAT inhibitor, tetrabenazine (10 μM; data not shown), on either DA_{cyt} or the number of surviving dopaminergic neurons (Figures 3C and 3D).

Methamphetamine and Cocaine

The discrepancy between the reduction of the total DA in reserpine-treated neurons and the lack of the effect of VMAT inhibition on DA_{cyt} might be explained by the distribution of synaptic vesicles between neuronal cell bodies and the neurites. If the majority of vesicles filled with DA are located in synaptic terminals far from the cell bodies, any transmitter redistributed from them would be invisible to IPE (see Experimental Procedures).

To examine the effects of other DA-releasing drugs on somatic DA concentration, we exposed L-DOPA-treated neurons to methamphetamine (METH), which disrupts the vesicular proton gradient and redistributes DA from synaptic vesicles to the cytosol (Sulzer et al., 2005). In contrast to the increased cytosolic catecholamine levels observed in chromaffin cells acutely treated with METH (Mosharov et al., 2003), neurons exposed to 50 μM

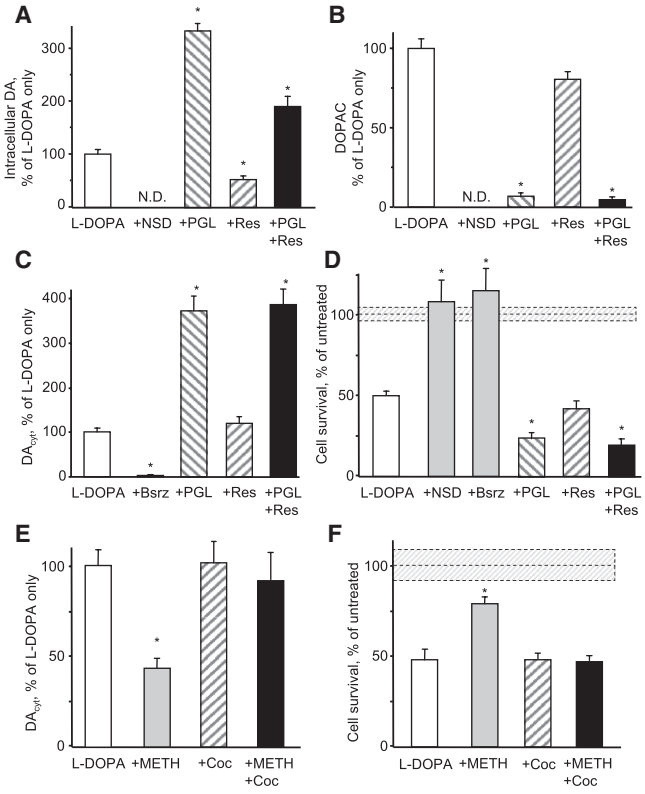

Figure 3. Effect of Pharmacological Inhibitors on DA_{cyt} and Neurotoxicity

(A and B) HPLC-EC measurements of total intracellular DA (A) and DOPAC (B) in rat VM neuronal cultures pretreated for 1 hr with 500 μM NSD-1015, 2 μM reserpine (Res), or 10 μM pargyline (PGL) and then treated with 100 μM L-DOPA for 1 hr (n = 6–10 dishes). N.D., not detected.

(C) DA_{cyt} in mouse VM neurons under the same treatments as above except for 2 μM benserazide (Bsrz) to block AADC (n = 22–81 cells).

(D) The effect of NSD-1015, benserazide, reserpine, and pargyline on the survival of mouse TH^+ neurons treated with 250 μM L-DOPA for 4 days (n = 6–20 dishes).

(E) DA_{cyt} concentration in TH-GFP neurons pretreated with 10 μM cocaine for 15 min, then exposed to 100 μM L-DOPA for 1 hr, and then treated with 50 μM METH for 15–30 min (n = 19–46 cells).

(F) Cell survival of mouse TH^+ neurons pretreated with METH and cocaine as in (E) and exposed to 250 μM L-DOPA for 4 days (n = 3–8 dishes).

*$p < 0.05$ versus cells treated with L-DOPA only by one-way ANOVA. Dotted lines and shadowed boxes in (D) and (F) represent mean ± SEM in untreated cells.

METH showed decreased DA_{cyt} (Figure 3E); 5 μM METH produced the same decrease of DA_{cyt} (38% of untreated cells; $p < 0.005$ by t test). METH-mediated reduction of DA_{cyt} was blocked by the DA uptake transporter (DAT) inhibitor cocaine, suggesting that the effect was due to reverse transport through DAT (Sulzer et al., 2005). METH-mediated decrease of DA_{cyt} and its blockade by cocaine were also observed in L-DOPA-treated cells in the presence of pargyline (data not shown). Note that DA_{cyt} in L-DOPA-treated neurons was unaffected by DAT inhibitors cocaine (Figure 3E) or nomifensine (5 μM; data not shown), supporting the idea that reverse transport is not induced by the elevated DA_{cyt} alone, but requires additional METH-mediated effects on DAT (Kahlig et al., 2005).

Consistent with the IPE results, METH protected neuronal cell bodies from L-DOPA toxicity (Figure 3F), despite the considerable neurite loss that occurs in METH-treated cultured DA neurons (Cubells et al., 1994; Larsen et al., 2002). When applied for 4 days without L-DOPA, neither METH or cocaine nor the combination of the two drugs had a significant effect on the number of surviving neurons (data not shown).

Genetic Manipulation of DA_{cyt} and Neurotoxicity

VMAT2 Overexpression

We previously developed a recombinant adenovirus that overexpresses VMAT2 (rVMAT2), resulting in reduced neuronal neuromelanin content and enhanced quantal size, and which increased the number of evoked quantal neurotransmitter release events from the terminals of cultured VM dopaminergic neurons (Pothos et al., 2000; Sulzer and Pothos, 2000). To investigate whether enhanced vesicular uptake may decrease DA_{cyt} and rescue neurons from L-DOPA-induced toxicity, we employed an adenoviral construct that resulted in overexpression of the recombinant VMAT2 in 80%–90% of both dopaminergic and nondopaminergic cells (Figure S2).

VMAT2 overexpression significantly decreased DA_{cyt} in L-DOPA-treated GFP^+ VM neurons (from 17.4 ± 1.7 μM, n = 74 neurons to 3.1 ± 0.8 μM, n = 28; Figure 4A), but had no effects on GFP^- neurons from the same culture (2.4 ± 0.8 μM, n = 33 versus 2.3 ± 1.9 μM, n = 7). GFP^+ neurons in cultures treated with a virus that did not contain rVMAT2 displayed the same DA_{cyt} levels after L-DOPA treatment as control cells (data not shown). Consistent with the kinetics of L-DOPA metabolic consumption (Figure 1), rVMAT2 lowered DA_{cyt} to the same extent in cells treated with 100 and 500 μM L-DOPA (Figure 4A). Moreover, infection with rVMAT2 effectively protected TH^+ neurons from the L-DOPA-mediated neurotoxicity (Figure 4B). It should be noted, however, that these data also suggest that somatic vesicles or other organelles that do not normally sequester substantial levels of DA can do so after transporter overexpression, as has been demonstrated for noncatecholaminergic AtT-20 cells (Pothos et al., 2000) and hippocampal neurons (Li et al., 2005).

α-Synuclein Knockout

To investigate the role of α-syn in mediating DA_{cyt} neurotoxicity, we generated α-syn-deficient mice that express eGFP in dopaminergic neurons (see Experimental Procedures). Whereas VM neurons from α-$syn^{-/-}$ and α-$syn^{+/-}$ mice were more resistant to L-DOPA-induced stress than neurons from their wild-type littermates (Figure 4C), IPE measurements indicated no difference in the DA_{cyt} concentration between the three groups (Figure 4D). These data suggest that the pathogenic effect of α-syn is downstream of DA synthesis (see Discussion), and that the presence of both elevated DA_{cyt} and α-syn is required for L-DOPA-induced neurotoxicity.

DA_{cyt} in SN and VTA Neurons

To address the question of differential susceptibility of neurons from different brain regions, we prepared cultures that were enriched with cells from either SN or VTA, as previously published (Burke et al., 1998). Immunolabeling for calbindin, a protein that is expressed at higher levels in VTA than in SN (Thompson et al., 2005), showed that in mixed VM cultures ~50% of TH^+ neurons were also $calbindin^+$, whereas the proportion of TH^+/$calbindin^+$ cells was ~85% in VTA cultures and ~25% in SN cultures (Figures 5A and 5B).

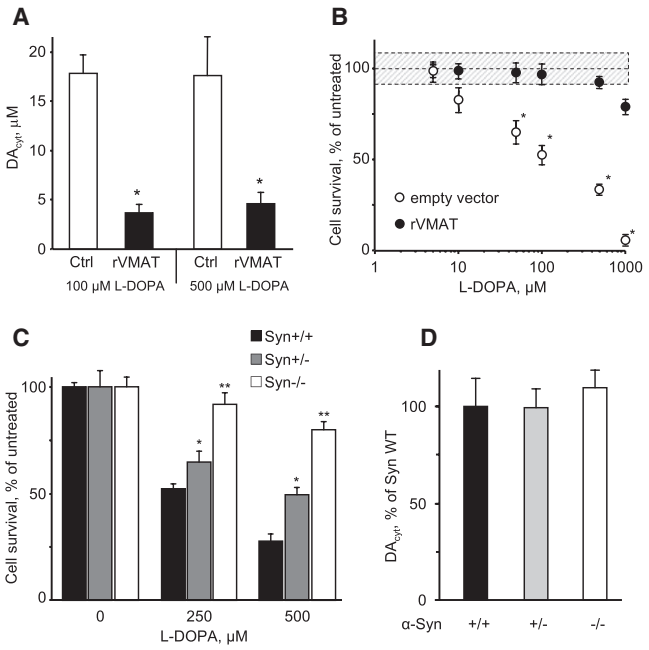

Figure 4. Effect of VMAT2 Overexpression and α-Syn Knockout on DA_{cyt} and Toxicity

(A) DA_{cyt} in sister cultures of mouse TH^+ neurons treated with L-DOPA for 1 hr; cells were either untransfected or were transfected with rVMAT2 or empty vector (not shown) 1 day before the application of L-DOPA. *p < 0.01 versus cells treated with L-DOPA only by one-way ANOVA (n = 15–28 cells).

(B) Neuroprotection of TH^+ neurons in rat VM cultures infected with rVMAT2 or empty vector and exposed to varying concentrations of L-DOPA on day 1 and assessed for survival on day 7. *p < 0.05 versus empty vector by two-way ANOVA.

(C) Reduced sensitivity of TH^+ neurons from α-syn-deficient mice to L-DOPA-induced neurotoxicity. Neurons from α-syn wild-type, heterozygous, and knockout littermate mice were treated with indicated L-DOPA concentrations for 4 days. *p < 0.05 and **p < 0.001 versus the wild-type by two-way ANOVA with Bonferroni post hoc test (n = 10–29 dishes).

(D) Comparison of DA_{cyt} levels in neurons from α-syn knockout, heterozygous, and wild-type mice treated with 100 μM L-DOPA for 1 hr (n = 20–49 cells).

IPE measurements showed that L-DOPA-treated SN neurons displayed 2- to 3-fold higher DA_{cyt} than VTA neurons (Figure 5C). This difference in DA_{cyt} translated into a significantly higher susceptibility of SN neurons to L-DOPA-induced toxicity, whereas VTA neurons were almost completely protected (Figure 5D). The resistance of VTA neurons to L-DOPA challenge was also seen in mixed VM cultures, where after 4 days of 250 μM L-DOPA the percentage of TH^+/$calbindin^+$ neurons increased from 52% to 88% ($p < 0.05$ by χ^2 test).

Relationship between Cytoplasmic Ca^{2+} and DA_{cyt}

The regulation of intracellular Ca^{2+} differs significantly between SN and VTA neurons (Gerfen et al., 1985; Surmeier, 2007; Thompson et al., 2005). Thus, to search for the mechanism that governs the difference in DA_{cyt} between the two neuronal

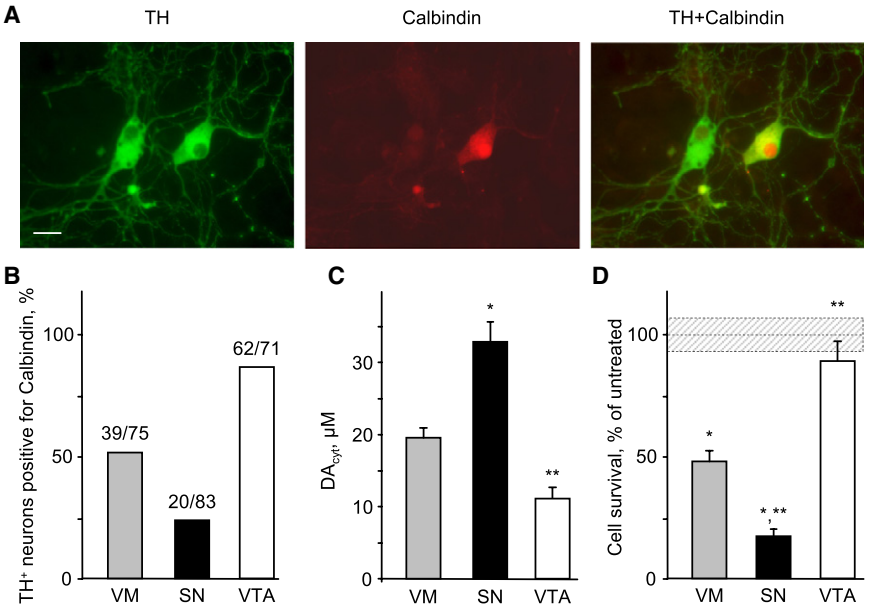

Figure 5. Sensitivity of SN and VTA DA Neurons to L-DOPA Challenge

(A) Representative images of VM neuronal cultures double stained for TH and calbindin. The scale bar represents 20 μm.

(B) Relative number of calbindin$^+$ cells within the population of TH$^+$ neurons.

(C) Cytosolic DA concentrations in VM, SN, and VTA TH$^+$ neurons treated with 100 μM L-DOPA for 1 hr. The representative experiment shown was repeated five times with 9–16 cells in each group in each experiment. $p < 0.01$ versus VM (*) or versus VM and SN (**) by one-way ANOVA.

(D) L-DOPA-induced neurotoxicity in cultures treated with 250 μM L-DOPA for 4 days. Dotted lines and shadowed boxes represent mean ± SEM in untreated cells. $p < 0.01$ versus untreated neurons of the same group (*) or versus L-DOPA-treated neurons of all other groups (**) by one-way ANOVA (n = 10–15 dishes).

populations, we investigated whether intracellular Ca^{2+} had an effect on L-DOPA-induced DA_{cyt} accumulation.

Cell pretreatment with the voltage-gated calcium channel blocker $CdCl_2$ or buffering cytoplasmic Ca^{2+} with the membrane-permeable chelator BAPTA-AM both significantly decreased DA_{cyt} in dopaminergic neurons from SN and VTA (Figure 6A). This suggests that the regulatory mechanism that links cytoplasmic Ca^{2+} and DA_{cyt} exists in both cell populations, and that the difference between SN and VTA neurons might be in the steady-state Ca^{2+} level. This would be consistent with SN neurons relying on dihydropyridine-sensitive L-type $Ca_V1.3$ channels for autonomous pacemaking, in contrast to VTA neurons that use Na^+ channels for pacemaking. Immunostaining of VM cultures for the α1D subunit of the L-type Ca^{2+} channels, which is specifically present in the $Ca_V1.3$ channels, showed that it expressed in both calbindin$^+$ and calbindin$^-$ DA neurons (Figure S3), consistent with previous reports (Rajadhyaksha et al., 2004; Striessnig et al., 2006). The $Ca_V1.2/Ca_V1.3$ blockers nimodipine (Figure 6A) and nitrendipine (not shown), however, had no effect on DA_{cyt} in L-DOPA exposed VTA neurons, but decreased DA_{cyt} in SN neurons to the levels found in VTA neurons (Figure S4). VM cultures treated with nimodipine were far more resistant to L-DOPA-induced neurodegeneration (Figure 6B). Pretreatment of SN neurons for 1 hr with the HCN channel antagonist ZD7288 (50 μM) or TTX (1 μM) had no significant effect on DA_{cyt} reached after L-DOPA treatment (data not shown).

To determine which enzyme or transporter is responsible for Ca^{2+}-induced upregulation of DA homeostasis, we first compared DA_{cyt} in SN and VTA neurons treated with pargyline and reserpine. DA_{cyt} was increased by the same percentile in both types of neurons (Figure 6C), suggesting that MAO and VMAT2 activities did not underlie the difference between DA_{cyt} handling by SN and VTA neurons and were not the regulatory targets. Next, DA_{cyt} in SN and VTA neuronal cultures was unaffected by the presence of the DAT blocker cocaine (data not shown). Finally, the uptake of L-DOPA in VM cultures pretreated with BAPTA-AM and benserazide was monitored by HPLC-EC and IPE in the amperometric detection mode, which in contrast to CV produces similar oxidative currents for DA and L-DOPA (Mosharov et al., 2003). Measurements by both methods demonstrated that L-DOPA uptake was unaffected by Ca^{2+} buffering (Figures 6D and 6E). Overall, our data suggest that MAO, VMAT, DAT, and the L-amino acid plasma transporter were not responsible for the difference in DA_{cyt} observed between SN and VTA neurons. Thus, it appears that the activity of AADC may provide the Ca^{2+}-sensitive metabolic step that leads to higher DA_{cyt} levels in SN neurons.

DISCUSSION

Efforts over the past decade have identified genes that cause familial instances of several neurodegenerative disorders, including Parkinson's disease. The steps underlying the degeneration of the specific neuronal populations associated with these diseases, however, have proven elusive. Here we show that selective death of SN dopaminergic neurons responsible for the definitive motor deficits in PD can result from a combination of multiple hits resulting from the activity of the L-type Ca^{2+} channels that create high cytoplasmic Ca^{2+} levels, an upregulation of DA_{cyt} synthesis by Ca^{2+}, and the presence of α-synuclein.

Dependence of Neurotoxicity on DA_{cyt}

A series of studies have suggested that dysregulation of DA_{cyt} maintenance underlies neuropathology in PD, but characterization of DA_{cyt} and its relationship to neurotoxicity has not been possible due to a lack of means to measure DA_{cyt}. We have adapted the recently introduced technique of IPE to characterize DA homeostasis in neuronal cytosol.

Our results confirm a relationship between high levels of DA_{cyt} and neurotoxicity. A variety of pharmacological and genetic

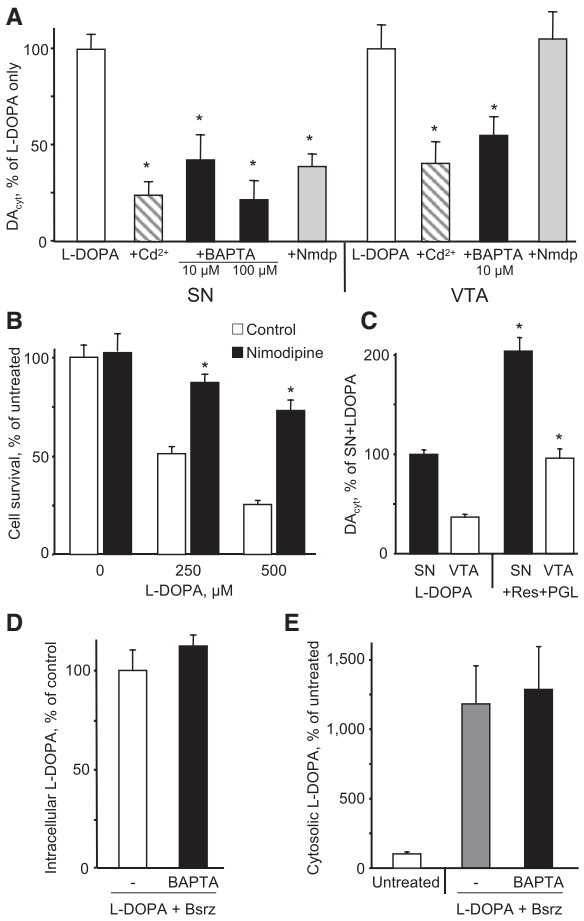

Figure 6. Regulation of DA_{cyt} by Cytoplasmic Ca^{2+}

(A) DA_{cyt} in SN and VTA neurons pretreated with 30 μM $CdCl_2$, 10 or 100 μM BAPTA-AM, or 10 μM nimodipine (Nmdp) for 1 hr, and then exposed to 100 μM L-DOPA for 1 hr. Data are presented as relative changes compared to SN and VTA neurons treated with L-DOPA only. *$p < 0.05$ versus L-DOPA only by one-way ANOVA (n = 11–52 cells).

(B) Protection of SN neurons from L-DOPA-induced neurotoxicity by the L-type Ca^{2+} channel blocker nimodipine (10 μM; 1 hr pretreatment). *$p < 0.05$ versus L-DOPA only by one-way ANOVA (n = 3–23 dishes).

(C) DA_{cyt} levels in SN and VTA neurons pretreated with 2 μM reserpine and 10 μM pargyline for 1 hr and then exposed to 100 μM L-DOPA for 1 hr. *$p < 0.05$ versus corresponding L-DOPA-only group by one-way ANOVA (n = 18–27 cells).

(D) Whole-cell L-DOPA concentration in VM cultures pretreated for 1 hr with 2 μM benserazide with and without 10 μM BAPTA-AM and then exposed to 100 μM L-DOPA for 1 hr (n = 4 dishes).

(E) Total cytosolic catechol concentrations (IPE in amperometric mode) in VM neurons either untreated or treated as in (D) (n = 10 cells).

means to influence DA homeostasis indicate that neurotoxicity was mediated by the cytosolic pool of DA, whereas other potential sources of cellular stress, including extracellular DA and L-DOPA, played limited roles under our experimental conditions. To compare the data from different experiments, we examined the dependence of cell survival on the integral of cell exposure to elevated DA levels (DA_{cyt} dose; Figure 7A; Figure S5). The relationship was close to linear, with doses above 100–200 μM·hr causing significant neurotoxicity. This finding was consistent over a wide variety of interventions that altered DA_{cyt} in different manners, including inhibition of L-DOPA conversion to DA, VMAT2 blockade or overexpression, and treatment with METH and cocaine. Cortical neurons were less resistant to L-DOPA challenge than midbrain DA neurons, although there are no reports of cell loss in the cortex of PD patients who received L-DOPA for many years. Conversely, VM neurons treated with the MAO inhibitor pargyline were significantly more resistant to DA_{cyt}-mediated toxicity (Figure 7A, asterisk). One possible explanation for the lower than expected levels of cell death observed in the presence of MAO blockade is a contribution of DA catabolic products that arise via MAO activity, that is, H_2O_2 and dihydroxyphenylacetaldehyde (DOPAL), as has been recently suggested (Burke et al., 2004; Eisenhofer et al., 2004). Although additional studies are required to characterize other factors that modulate susceptibility of neurons to stress, our data support the exploration of central MAO inhibitors as treatments for PD either as monotherapy at early stages of the disease or in combination with L-DOPA in the advanced disease stages (Chen et al., 2007; Hauser et al., 2008); in both cases, MAO blockers would increase the availability of DA_{cyt} for vesicular sequestration while preventing the buildup of toxic DA metabolites.

DA_{cyt} Maintenance in Neuronal Somas and Synaptic Terminals

Perhaps surprisingly, reserpine and METH, drugs that disrupt vesicular DA sequestration, did not increase DA_{cyt}, despite the depletion of vesicular DA stores evident from HPLC-EC measurements of the total intracellular DA (Figure 3; Larsen et al., 2002). These results are, however, consistent with diffusion calculations, indicating that IPE measures only DA in the cell body (see Experimental Procedures), that is, the number of DA storage vesicles in the soma might be insufficient to detectably increase DA_{cyt} following reserpine or METH. Although some DA secretory organelles reside in or close to neuronal cell bodies, as evident from somatodendritic vesicular DA release from midbrain neurons (Jaffe et al., 1998; Rice et al., 1997), emptying one synaptic vesicle containing 10,000 DA molecules (Pothos et al., 1998) would increase DA_{cyt} by only 0.01 μM (see Experimental Procedures), and 150–200 such vesicles would need to be emptied to produce a 10% increase over the 15–20 μM DA_{cyt} observed in L-DOPA-treated cells. In comparison, adrenal chromaffin cells, which lack neurites and are filled with secretory vesicles that each contain ~1,000,000 transmitter molecules (Wightman et al., 1991), show increased cytosolic catechol concentrations following reserpine or METH (Mosharov et al., 2003). Although IPE cannot measure DA_{cyt} in axonal terminals, it is possible that a similarly large increase in DA_{cyt} occurs in METH-treated neuronal terminals and, if so, this may explain the unusual pattern of METH-induced neurodegeneration in which neurites but not cell bodies are damaged in vitro (Cubells et al., 1994; Larsen et al., 2002), in animal models in vivo (Ricaurte et al., 1982), and in imaging studies of METH abusers after prolonged abstinence (Chang et al., 2007). Postmortem examination of chronic METH users reveals a more severe DA axonal loss in

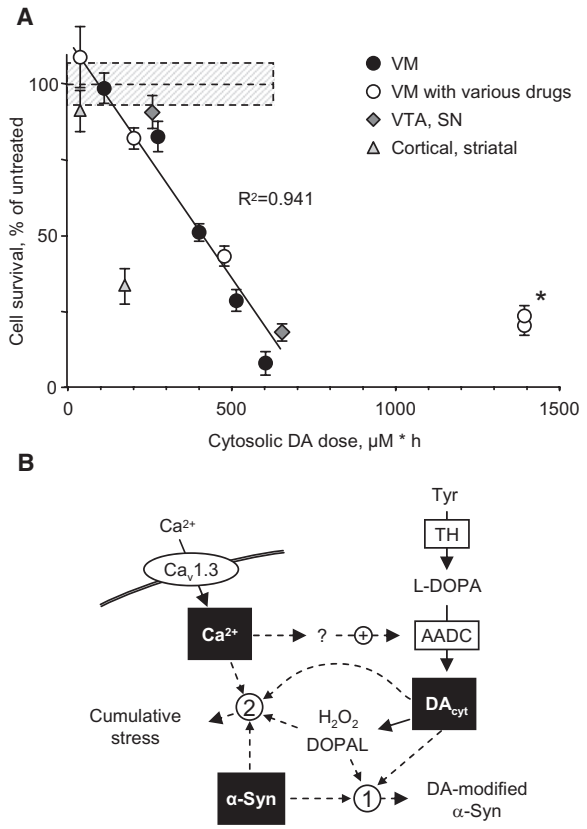

Figure 7. DA_{cyt} Dose and Neurotoxicity

(A) Dependence of cell survival under L-DOPA-induced stress on the DA_{cyt} dose in mouse neurons. DA_{cyt} dose was estimated as $[DA_{cyt}]\cdot T_{Exposure} = [DA_{cyt}]\cdot Ln([L\text{-}DOPA]/K_{0.5})/k$, where $[DA_{cyt}]$ is the concentration of cytosolic DA in cells treated with a saturating level (>50 μM) of L-DOPA for 1 hr, [L-DOPA] is the initial drug concentration, and $K_{0.5}$ = 9.7 μM and k = 0.15 hr^{-1} are the kinetic constants derived from Figures 1B and 1E, respectively. $T_{Exposure}$ therefore approximates the time during which extracellular L-DOPA remained higher than $K_{0.5}$ (Figure 1F). The data points are (from left to right): filled circles: VM cultures treated with 25, 100, 250, 500, and 1000 μM L-DOPA alone; open circles: VM neurons treated with 250 μM L-DOPA in the presence of benserazide, METH, reserpine, PGL, and PGL + reserpine; diamonds: VTA and SN neurons; and triangles: striatal and cortical neurons treated with 250 μM L-DOPA. Dotted lines and shadowed boxes represent mean ± SEM in untreated cells. The solid line is the linear fit of all data points, excluding striatal and cortical neurons, and two data points indicated by an asterisk. Treatments to the right of this line are neuroprotective, as the same level of cell death is achieved with higher DA_{cyt} doses; treatments to the left of the line are more susceptible to DA_{cyt} stress.

(B) Multi-hit model of PD pathogenesis. Neurotoxicity is a result of multiple factors, including the presence of α-syn, elevation of cytoplasmic Ca^{2+}, and the buildup of DA_{cyt} and its metabolites. Nonexclusive toxic steps may result from (1) mechanisms that require direct interaction between DA or its metabolites with α-syn, such as DA-modified stabilization of α-syn protofibrils or inhibition of chaperone-mediated autophagy, or (2) cumulative damage from multiple independent sources. Decreasing the levels of any of the three players provides neuroprotection.

the caudate than in the putamen, presumably explaining the lack of parkinsonian symptoms in METH abusers (Moszczynska et al., 2004).

Upregulation of DA Homeostasis by Ca^{2+} Explains Higher Vulnerability of SN Neurons to L-DOPA-Induced Stress

We found that DA_{cyt} reached in L-DOPA-treated dopaminergic neurons directly correlated with intracellular Ca^{2+}, as lower DA_{cyt} levels were found in SN and VTA neurons following voltage-gated calcium channel blockade by $CdCl_2$ or cytoplasmic Ca^{2+} buffering by BAPTA-AM. Conversely, significantly higher DA_{cyt} was reached in SN than in VTA neurons, consistent with the pacemaking activity of dihydropyridine-sensitive $Ca_v1.3$ channels in SN but not VTA neurons. Notably, although dihydropyridines nimodipine and nitrendipine had no effect on DA_{cyt} concentration in VTA neurons, they decreased DA_{cyt} in SN neurons to the levels in the VTA, and provided neuroprotection from L-DOPA-induced cell death.

The target of Ca^{2+}-dependent upregulation of DA homeostasis appears to be the conversion of L-DOPA to DA by AADC. Although regulation of AADC activity via protein kinase A- and C-mediated phosphorylation has been reported (Duchemin et al., 2000; Young et al., 1998), these mechanisms require further characterization, as $Ca_v1.3$ channels are also regulated by these second-messenger pathways (Baroudi et al., 2006; Rajadhyaksha and Kosofsky, 2005). It should also be noted that Ca^{2+}-dependent phosphorylation of TH (Dunkley et al., 2004) is likely to play a role in the absence of exogenously added L-DOPA.

A Multiple-Hit Hypothesis of SN Neurodegeneration in PD

Multiple genes have been identified to cause familial PD, but the disease may require multiple steps, such as an initial insult together with an insufficient stress response (Abou-Sleiman et al., 2006; Conway et al., 2001; LaVoie et al., 2005; Martinez-Vicente et al., 2008; Moore et al., 2005; Sang et al., 2007; Sulzer, 2007), which may explain why known genetic and environmental factors do not straightforwardly account for idiopathic PD. The interaction between high DA_{cyt} and α-syn may provide one of the multiple-hit mechanisms. Due to the presence of α-syn in Lewy bodies and the role of α-syn mutations or gene multiplication in some forms of familial PD, it is widely believed that this protein plays a central role in the degeneration of VM DA neurons. Consistent with previous reports that dopaminergic neurons in α-syn deficient mice show reduced susceptibility to neurotoxins (Alvarez-Fischer et al., 2008; Dauer et al., 2002), we found that α-syn deletion makes VM neurons resistant to L-DOPA-induced toxicity. By contrast, neuronal DA_{cyt} was unaffected by the absence of α-syn (Figure 4D), similar to cytosolic catecholamine levels in chromaffin cells from α-syn null animals (Mosharov et al., 2006). These data are consistent with a toxic mechanism downstream of DA synthesis that may involve stabilization of toxic α-syn protofibrils by DA, inhibition of chaperone-mediated autophagy by DA-modified α-syn, or a cumulative stress from various sources, which, in addition to DA_{cyt}, Ca^{2+}, and α-syn, may include mitochondrial and proteasomal dysfunction and inflammatory responses (Figure 7B) (Burke et al., 2008; Conway et al., 2001; Dauer and Przedborski, 2003; Gao et al., 2008; Martinez-Vicente et al., 2008; Ved et al., 2005). Additionally, although normal expression levels of mouse wild-type α-syn do not seem to affect DA_{cyt} concentration, α-syn mutation

or overexpression may lead to elevated DA_{cyt} (Lotharius et al., 2002; Mosharov et al., 2006) that would further exacerbate neurotoxicity.

It is striking that L-DOPA doses that produced neurotoxicity in this study also induce the synthesis of neuromelanin (Sulzer et al., 2000), an autophagosome containing oxidized dopamine products (Sulzer et al., 2008). Moreover, VMAT2 overexpression, which as we show here decreased DA_{cyt} and abolished L-DOPA-induced neuronal death, has also been demonstrated to inhibit neuromelanin synthesis (Sulzer et al., 2000). Together, these data support the idea that neuromelanin synthesis is a stress response and that the presence of neuromelanin in human SN and its accumulation over time are indicative of an ongoing DA_{cyt} damage even in normal non-PD human brain. Conversely, dopaminergic neurons in the VTA, which are spared in PD, produce minimal neuromelanin over a lifetime (Hirsch et al., 1988; Liang et al., 2004; Zecca et al., 2001).

Whereas DA neurons are comparatively resistant to DA_{cyt} toxicity, it remains unclear whether neurotoxic DA_{cyt} levels are reached in humans, particularly during treatment of PD patients with L-DOPA. Although L-DOPA therapy is linked to increased levels of the products of peroxynitrite-mediated oxidative stress in cerebrospinal fluid (CSF) (Isobe et al., 2006) and a more rapid decline in striatal dopamine transporter over the course of L-DOPA therapy, there is no increase in the rate of symptomatic progression in PD patients with L-DOPA (Fahn, 2005). Moreover, whereas recent reports demonstrate L-DOPA-induced neurotoxicity in rodents (Chen et al., 2008; Jeon et al., 2007), other in vivo studies found L-DOPA to be benign or even neuroprotective (reviewed by Olanow et al., 2004). Important factors may include the ability of L-DOPA-induced mild oxidative stress to activate glutathione synthesis (Han et al., 1996; Mena et al., 1997) and induce macroautophagy (Sulzer et al., 2008), and a likely protective action of L-DOPA therapy on the striatopallidal pathway (Day et al., 2006). Normal L-DOPA concentration in the CSF is only ~5 nM (Tohgi et al., 1997) and increases to ~300 nM in L-DOPA-treated patients (Tohgi et al., 1995), which is likely within a range that cellular stress response pathways can handle. It should be emphasized that the meaning of our findings is not that L-DOPA is neurotoxic to humans, as it is artificially used as a tool to enhance DA: genuine PD does not result from L-DOPA exposure, but may result following chronically elevated DA_{cyt} and the presence of other genetic and environmental hits.

The newly identified relationship between high Ca^{2+} and DA_{cyt} may underlie the selective vulnerability of dopaminergic neurons in SN and locus coeruleus, a group of noradrenergic neurons that also rely on Ca^{2+} channel pacemaking (Williams et al., 1984). If so, various strategies could be employed to prevent neuronal death in PD, including an inhibition of $Ca_v1.3$ channel activity (Surmeier, 2007) or blocking the deleterious effects of DA-protein interactions (Martinez-Vicente et al., 2008). By contrast, symptomatic treatment of PD relies on therapies that enhance synaptic vesicle sequestration of DA, thereby reconstituting the dopaminergic tone in the striatum. As discussed above, our data may indicate advantages to using central MAO inhibitors as PD drugs. Likewise, as we show here, VMAT2 overexpression enhances exocytotic DA release while decreasing DA_{cyt}. Because VMAT2 overexpression not only promotes DA neurotransmission in a manner similar to L-DOPA but also confers neuroprotection, controlled VMAT2 overexpression may provide a therapeutic intervention for PD, either alone or in combination with L-DOPA or MAO blockers.

EXPERIMENTAL PROCEDURES

Mouse Strains

For neurotoxicity and IPE experiments, neurons from C57/Bl6 mice or from transgenic mice that express green fluorescent protein (TH-GFP$^{+/-}$) under the control of the rat tyrosine hydroxylase (TH) promoter (Sawamoto et al., 2001) were used. α-synuclein null mice that express eGFP under the control of TH promoter were generated in two steps. TH-GFP$^{+/-}$ mice were crossed with α-syn$^{-/-}$ mice (strain B6;129X1-Snca^{tm1Rosl}/J from Jackson Labs; originally from Abeliovich et al., 2000). Next, the resulting TH-GFP$^{+/-}$/α-syn$^{+/-}$ mice were crossed with each other and genotyped for the presence of both eGFP and α-syn to obtain TH-GFP$^{+/-}$/α-syn$^{+/-}$, TH-GFP$^{+/-}$/α-syn$^{-/-}$, and TH-GFP$^{+/-}$/α-syn$^{+/+}$ littermates. For HPLC measurements, cells from Sprague-Dawley rats were used. Animals were used in accordance with the National Institutes of Health guidelines for the use of live animals, and the animal protocol was approved by the Institutional Animal Care and Use Committee of Columbia University.

Primary Neuronal Cultures

Ventral midbrain (VM), cortical, or striatal neurons from postnatal day 0–2 mice or rats were dissected, dissociated, and plated on a monolayer of cortical astrocytes at the plating density of ~100,000 cells/cm^2, as previously described (Burke et al., 1998; Rayport et al., 1992). Mouse neurons were cultured on glass poly-D-lysine-coated coverslips attached to ~0.8 cm^2 wells cut into 50 mm dishes. Rat neurons were cultured on 35 mm tissue culture dishes (~9.6 cm^2).

We previously reported (Mena et al., 1997) that lower levels of L-DOPA provided a short-lasting enhancement of dopaminergic neuron survival due to neuroprotective antioxidant responses to L-DOPA-induced oxidative stress. We have since demonstrated that glial-derived neurotrophic factor (GDNF) is selectively neuroprotective for postnatally derived dopaminergic neurons, providing markedly enhanced survival (Burke et al., 1998), and now routinely include this component in the culture medium. As shown in the present study, L-DOPA is not neuroprotective in the presence of GDNF (Figure 2A), presumably because the neuroprotective response has been occluded, allowing the toxic response to be revealed.

Experiments were conducted 6–10 days postplating; all treatments were performed at 37°C. Pseudo-3D images of cultured TH-GFP neurons (Figure S1) were obtained with a two-photon microscope (Zeiss Axioskop2 FS MOT upright microscope, LSM 510 Coherent two-photon setup; Carl Zeiss MicroImaging, Thornwood, NY, USA), using 850 nm excitation and 525 nm emission wavelengths. Z sections were taken at 1 μm increments. Other images were acquired on a conventional fluorescence microscopy setup (Zeiss Axiovert 100 microscope) equipped with a Zeiss AxioCam MRm camera and FITC and rhodamine filter sets (Chroma, Rockingham, VT, USA).

Adenoviral Vector Construction and Transfection of Neurons with rVMAT2

A hemagglutinin (HA) -tagged VMAT2 cDNA was first subcloned into the shuttle vector pTet-EF, then coinfected with donor virus DNA (φ5) into HEK293 cells expressing Cre recombinase, and the resultant VMAT2-HA-harboring adenovirus was purified and stored as previously described at ~8000 pfu/μl (Krantz et al., 1997). Primary rat VM cultures were incubated with 1 μl of rVMAT2 diluted in 100 μl of media for 5 hr and then 2 ml of media was added to each dish; φ5 alone was used as a negative (empty virus) control. Transfection efficiency was 80%–90% for both dopaminergic and GABAergic neuronal types (Figure S2).

Immunocytochemistry and Western Blots

Immunostaining of 4% paraformaldehyde-fixed cultures was performed using mouse or rabbit anti-TH (1:1000; Chemicon, Temecula, CA, USA), rabbit

anti-MAP2 (1:500; Chemicon), and mouse anti-calbindin D-28K (1:200; Sigma, St. Louis, MO, USA) antibodies, followed by secondary antibodies conjugated with Alexa 488 or Alexa 594 (1:200; Molecular Probes, Eugene, OR, USA). Polyclonal rabbit anti-VMAT2 antibody (1:200; Pel-Freez Biologicals, Rogers, AR, USA) was used to detect endogenous and exogenous VMAT2 protein. For immunodetection of HA-tagged rVMAT2, cultures were stained using monoclonal anti-HA antibody (1:200; BabCO, Richmond, CA, USA) (Pothos et al., 2000). Western immunoanalysis of VMAT2 protein was performed as described (Krantz et al., 1997) with VMAT2 antibody (1:500; Chemicon), horseradish peroxidase-conjugated secondary antibody, and visualization by enhanced chemiluminescence (Pierce Biotech, Rockford, IL, USA).

Neurotoxicity

Cells were preincubated with rVMAT2 for 1 day and with various DA metabolism inhibitors for 1 hr before the application of L-DOPA, unless stated otherwise. Following 1–7 days of incubation, neuronal cultures were fixed and stained for TH (VM neurons) or MAP2 (cortical and striatal neurons). The total numbers of immunoreactive neurons were then tallied and analyzed as previously described (Larsen et al., 2002). Alternatively, neuronal density was assessed by counting the number of immunoreactive cells in 24 fields of view at 200× magnification (Plan-Neofluar 20× objective; ~0.8 mm^2 viewing field) and taking the average as a representative for each dish. Although the two methods yielded similar results, the second approach was more robust, producing lower deviation within experimental groups. The counts were performed by an observer blind to the experimental treatments.

High-Performance Liquid Chromatography with Electrochemical Detection

Whole-cell DA, dihydroxyphenylacetic acid (DOPAC), and L-DOPA levels were determined by HPLC-EC as previously described (Feigin et al., 2001; Larsen et al., 2002). DA, DOPAC, and L-DOPA amounts were calculated from areas under HPLC peaks using calibration curves and normalized to protein concentrations in each sample.

Intracellular Patch Electrochemistry

Measurements of cytosolic DA (DA_{cyt}) concentrations in neurons were based on protocols for PC12 cells and chromaffin cells (Mosharov et al., 2003, 2006). A polyethylene-coated 5 μm carbon fiber electrode (CFE) was placed inside a glass patch pipette and used in cyclic voltammetric (CV) mode of detection where voltage ramps from −450 mV holding potential to +800 mV and back to −450 mV over 10 ms (scan rate of 250 mV/ms) were applied at 100 ms intervals. After achieving a seal between the cell and the patch pipette, the plasma membrane was ruptured by suction and substances diffusing from the cytosol into the pipette were observed as a slow wave of oxidation current. As no difference was found between IPE signals using intracellular and extracellular ionic compositions as the patch pipette saline (Mosharov et al., 2003), the same saline was employed as the bath and the pipette solutions in the present study. The saline contained (in mM): 118 NaCl, 2.5 KCl, 2 $MgCl_2$, 2 $CaCl_2$, 1 NaH_2PO_4, 10 glucose, 25 HEPES-NaOH (pH 7.4); the same concentrations of all drugs, including L-DOPA, were present in the bath and in the patch pipette. After background current subtraction, the concentration of DA at the pipette tip was calculated as previously described (Mosharov et al., 2003). IPE sensitivity, estimated as the current 3-fold higher than the root mean square of the noise on the subtraction voltammogram, was ~100 nM DA; the calibration curves were log-linear for up to at least 1 mM DA concentration (Mosharov et al., 2003). The initial concentration of DA_{cyt} was calculated using neuronal cell-body volume, and the volume of the pipette tip was estimated from photographs taken before each recording (Figure S1).

To investigate whether the electrode sensitivity for DA was affected by the presence of compounds present in the recording media, we performed a series of calibration measurements of 5 μM DA with and without the drugs (Table S1). Based on these data, NSD-1015 cannot be used for IPE experiments because it abolished the oxidation signal of DA.

Although CV voltammograms cannot differentiate between DA, L-DOPA, and the product of DA catabolism, DOPAC, there are several reasons to suspect that DA represented the majority of the cytosolic oxidation signal estimated by IPE. First, the sensitivity of CV is 15- to 20-fold higher for DA molecules than for other catechols (Mosharov et al., 2003). Second, there were identical concentrations of L-DOPA present in the patch pipette and extracellular saline during the recordings; thus, any change in the oxidation signal after achieving the whole-cell configuration could not be due to the influx of L-DOPA into the patch pipette per se. Third, L-DOPA is rapidly converted to DA once in the cytosol, and enhanced DA can be measured in these cultures within 90 s (Pothos et al., 1998), whereas, as shown in Results, inhibition of AADC almost completely abolished the oxidation signal from L-DOPA-treated cells. Finally, neither L-DOPA nor DOPAC are VMAT2 substrates, arguing against a possibility that the observed decrease in the cytosolic signal in neurons overexpressing VMAT2 was due to nonspecific catechol uptake into the vesicles.

To estimate the contribution of neurotransmitter from neurites to the CV oxidation signal, we calculated the time required for DA to diffuse into the cell body and then into the patch pipette. The average neuronal soma diameter and the distance from the cell to the CFE measured from photographs acquired before the recordings were 17.3 ± 3.9 μm and 16.6 ± 3.9 μm, respectively. Diffusion time (t) was calculated as $t = x^2/2D$, where x is the distance and D is the DA diffusion coefficient, $2.7*10^{-6}$ cm^2/s (Nicholson, 1999). It follows that DA from the middle of the cell body (x = 25.3 μm) would reach the CFE in 1.2 s, which was close to the average time to oxidation peak maximum experimentally observed in IPE recordings (1.4 ± 0.8 s, mean ± SEM, n = 34 neurons; Figure S1). In contrast, it would take approximately ten times longer for DA to diffuse from a varicosity positioned three cell-body diameters away (x = 77.1 μ); this delay would be longer still if the shape and diffusional barriers within the neurite were taken into account. We conclude that the majority of DA measured by IPE represents neurotransmitter that resided within the neuronal soma.

Possible Influence of Vesicular DA Cargo on the DA_{cyt} Measurements

If one synaptic vesicle releases all its content inside the neuronal soma, the change in the DA_{cyt} concentration will equal $Q_N/N_A/V_{cell}$, where Q_N is vesicular quantal size (~10,000 molecules in L-DOPA-treated neuronal synaptic vesicles; Pothos et al., 1998), N_A is Avogadro's Constant ($6.023*10^{23}$ molecules/mol), and V_{cell} is the cell-soma volume (~1.77 pl for a cell with a diameter of 15 μm). It follows that emptying one vesicle would increase DA_{cyt} by 10 nM, although this value might be underestimated because the effective cytosolic volume is smaller due to the presence of other organelles. In a similar scenario inside a synaptic terminal (~1 μm in diameter), DA_{cyt} will be increased by >30 μM.

Statistical Analyses

Statistical analysis was performed in Prism 4 (GraphPad Software, La Jolla, CA, USA), using one-way analysis of variance (ANOVA) followed by Tukey's post hoc test for comparisons across multiple groups or two-way ANOVA with Bonferroni post test for the paired data.

SUPPLEMENTAL DATA

Supplemental data include five figures and a table and can be found with this article online at http://www.neuron.org/supplemental/S0896-6273(09)00166-4.

ACKNOWLEDGMENTS

This article is dedicated to Barbara and Jeffry Picower, whose own dedication to this and other projects have provided extraordinary support and inspiration. We thank the Picower Foundation, the Parkinson's Disease Foundation, the National Parkinson Foundation, NINDS Udall Center of Excellence, and NIDA for support.

Accepted: January 24, 2009
Published: April 29, 2009

REFERENCES

Abeliovich, A., Schmitz, Y., Farinas, I., Choi-Lundberg, D., Ho, W.H., Castillo, P.E., Shinsky, N., Verdugo, J.M., Armanini, M., Ryan, A., et al. (2000). Mice lacking α-synuclein display functional deficits in the nigrostriatal dopamine system. Neuron *25*, 239–252.

Abou-Sleiman, P.M., Muqit, M.M., and Wood, N.W. (2006). Expanding insights of mitochondrial dysfunction in Parkinson's disease. Nat. Rev. Neurosci. *7*, 207–219.

Alvarez-Fischer, D., Henze, C., Strenzke, C., Westrich, J., Ferger, B., Hoglinger, G.U., Oertel, W.H., and Hartmann, A. (2008). Characterization of the striatal 6-OHDA model of Parkinson's disease in wild type and α-synuclein-deleted mice. Exp. Neurol. *210*, 182–193.

Baroudi, G., Qu, Y., Ramadan, O., Chahine, M., and Boutjdir, M. (2006). Protein kinase C activation inhibits $Ca_v1.3$ calcium channel at NH_2-terminal serine 81 phosphorylation site. Am. J. Physiol. Heart Circ. Physiol. *291*, H1614–H1622.

Burke, R.E., Antonelli, M., and Sulzer, D. (1998). Glial cell line-derived neurotrophic growth factor inhibits apoptotic death of postnatal substantia nigra dopamine neurons in primary culture. J. Neurochem. *71*, 517–525.

Burke, W.J., Li, S.W., Chung, H.D., Ruggiero, D.A., Kristal, B.S., Johnson, E.M., Lampe, P., Kumar, V.B., Franko, M., Williams, E.A., and Zahm, D.S. (2004). Neurotoxicity of MAO metabolites of catecholamine neurotransmitters: role in neurodegenerative diseases. Neurotoxicology *25*, 101–115.

Burke, W.J., Kumar, V.B., Pandey, N., Panneton, W.M., Gan, Q., Franko, M.W., O'Dell, M., Li, S.W., Pan, Y., Chung, H.D., and Galvin, J.E. (2008). Aggregation of α-synuclein by DOPAL, the monoamine oxidase metabolite of dopamine. Acta Neuropathol. *115*, 193–203.

Caudle, W.M., Colebrooke, R.E., Emson, P.C., and Miller, G.W. (2008). Altered vesicular dopamine storage in Parkinson's disease: a premature demise. Trends Neurosci. *31*, 303–308.

Chan, C.S., Guzman, J.N., Ilijic, E., Mercer, J.N., Rick, C., Tkatch, T., Meredith, G.E., and Surmeier, D.J. (2007). 'Rejuvenation' protects neurons in mouse models of Parkinson's disease. Nature *447*, 1081–1086.

Chang, L., Alicata, D., Ernst, T., and Volkow, N. (2007). Structural and metabolic brain changes in the striatum associated with methamphetamine abuse. Addiction *102*, 16–32.

Chen, J.J., Swope, D.M., and Dashtipour, K. (2007). Comprehensive review of rasagiline, a second-generation monoamine oxidase inhibitor, for the treatment of Parkinson's disease. Clin. Ther. *29*, 1825–1849.

Chen, L., Ding, Y., Cagniard, B., Van Laar, A.D., Mortimer, A., Chi, W., Hastings, T.G., Kang, U.J., and Zhuang, X. (2008). Unregulated cytosolic dopamine causes neurodegeneration associated with oxidative stress in mice. J. Neurosci. *28*, 425–433.

Chien, J.B., Wallingford, R.A., and Ewing, A.G. (1990). Estimation of free dopamine in the cytoplasm of the giant dopamine cell of *Planorbis corneus* by voltammetry and capillary electrophoresis. J. Neurochem. *54*, 633–638.

Clayton, D.F., and George, J.M. (1998). The synucleins: a family of proteins involved in synaptic function, plasticity, neurodegeneration and disease. Trends Neurosci. *21*, 249–254.

Colliver, T., Hess, E., Pothos, E.N., Sulzer, D., and Ewing, A.G. (2000). Quantitative and statistical analysis of the shape of amperometric spikes recorded from two populations of cells. J. Neurochem. *74*, 1086–1097.

Conway, K.A., Rochet, J.C., Bieganski, R.M., and Lansbury, P.T., Jr. (2001). Kinetic stabilization of the α-synuclein protofibril by a dopamine-α-synuclein adduct. Science *294*, 1346–1349.

Cubells, J.F., Rayport, S., Rajendran, G., and Sulzer, D. (1994). Methamphetamine neurotoxicity involves vacuolation of endocytic organelles and dopamine-dependent intracellular oxidative stress. J. Neurosci. *14*, 2260–2271.

Dauer, W., and Przedborski, S. (2003). Parkinson's disease: mechanisms and models. Neuron *39*, 889–909.

Dauer, W., Kholodilov, N., Vila, M., Trillat, A.C., Goodchild, R., Larsen, K.E., Staal, R., Tieu, K., Schmitz, Y., Yuan, C.A., et al. (2002). Resistance of α-synuclein null mice to the parkinsonian neurotoxin MPTP. Proc. Natl. Acad. Sci. USA *99*, 14524–14529.

Day, M., Wang, Z., Ding, J., An, X., Ingham, C.A., Shering, A.F., Wokosin, D., Ilijic, E., Sun, Z., Sampson, A.R., et al. (2006). Selective elimination of glutamatergic synapses on striatopallidal neurons in Parkinson disease models. Nat. Neurosci. *9*, 251–259.

Duchemin, A.M., Berry, M.D., Neff, N.H., and Hadjiconstantinou, M. (2000). Phosphorylation and activation of brain aromatic L-amino acid decarboxylase by cyclic AMP-dependent protein kinase. J. Neurochem. *75*, 725–731.

Dunkley, P.R., Bobrovskaya, L., Graham, M.E., von Nagy-Felsobuki, E.I., and Dickson, P.W. (2004). Tyrosine hydroxylase phosphorylation: regulation and consequences. J. Neurochem. *91*, 1025–1043.

Edwards, R.H. (1993). Neural degeneration and the transport of neurotransmitters. Ann. Neurol. *34*, 638–645.

Eisenhofer, G., Kopin, I.J., and Goldstein, D.S. (2004). Catecholamine metabolism: a contemporary view with implications for physiology and medicine. Pharmacol. Rev. *56*, 331–349.

Fahn, S. (2005). Does levodopa slow or hasten the rate of progression of Parkinson's disease? J. Neurol. *252*, IV37–IV42.

Feigin, A., Fukuda, M., Dhawan, V., Przedborski, S., Jackson-Lewis, V., Mentis, M.J., Moeller, J.R., and Eidelberg, D. (2001). Metabolic correlates of levodopa response in Parkinson's disease. Neurology *57*, 2083–2088.

Gao, H.-M., Kotzbauer, P., Uryu, K., Leight, S., Trojanowski, J., and Lee, V. (2008). Neuroinflammation and oxidation/nitration of α-synuclein linked to dopaminergic neurodegeneration. J. Neurosci. *28*, 7687–7698.

Gerfen, C.R., Baimbridge, K.G., and Miller, J.J. (1985). The neostriatal mosaic: compartmental distribution of calcium-binding protein and parvalbumin in the basal ganglia of the rat and monkey. Proc. Natl. Acad. Sci. USA *82*, 8780–8784.

Han, S.K., Mytilineou, C., and Cohen, G. (1996). L-DOPA up-regulates glutathione and protects mesencephalic cultures against oxidative stress. J. Neurochem. *66*, 501–510.

Hauser, R.A., Lew, M.F., Hurtig, H.I., Ondo, W.G., Wojcieszek, J., and Fitzer-Attas, C.J. (2008). Long-term outcome of early versus delayed rasagiline treatment in early Parkinson's disease. Mov. Disord., in press. Published online December 11, 2008. 10.1002/mds.22402.

Hirsch, E., Graybiel, A.M., and Agid, Y.A. (1988). Melanized dopaminergic neurons are differentially susceptible to degeneration in Parkinson's disease. Nature *334*, 345–348.

Isobe, C., Abe, T., Kikuchi, T., Murata, T., Sato, C., and Terayama, Y. (2006). Cabergoline scavenges peroxynitrite enhanced by L-DOPA therapy in patients with Parkinson's disease. Eur. J. Neurol. *13*, 346–350.

Jaffe, E.H., Marty, A., Schulte, A., and Chow, R.H. (1998). Extrasynaptic vesicular transmitter release from the somata of substantia nigra neurons in rat midbrain slices. J. Neurosci. *18*, 3548–3553.

Jeon, M.Y., Lee, W.Y., Kang, H.Y., and Chung, E.J. (2007). The effects of L-3,4-dihydroxyphenylalanine and dopamine agonists on dopamine neurons in the progressive hemiparkinsonian rat models. Neurol. Res. *29*, 289–295.

Kahlig, K.M., Binda, F., Khoshbouei, H., Blakely, R.D., McMahon, D.G., Javitch, J.A., and Galli, A. (2005). Amphetamine induces dopamine efflux through a dopamine transporter channel. Proc. Natl. Acad. Sci. USA *102*, 3495–3500.

Krantz, D.E., Peter, D., Liu, Y., and Edwards, R.H. (1997). Phosphorylation of a vesicular monoamine transporter by casein kinase II. J. Biol. Chem. *272*, 6752–6759.

Larsen, K.E., Fon, E.A., Hastings, T.G., Edwards, R.H., and Sulzer, D. (2002). Methamphetamine-induced degeneration of dopaminergic neurons involves autophagy and upregulation of dopamine synthesis. J. Neurosci. *22*, 8951–8960.

LaVoie, M.J., Ostaszewski, B.L., Weihofen, A., Schlossmacher, M.G., and Selkoe, D.J. (2005). Dopamine covalently modifies and functionally inactivates parkin. Nat. Med. *11*, 1214–1221.

Li, H., Waites, C.L., Staal, R.G., Dobryy, Y., Park, J., Sulzer, D.L., and Edwards, R.H. (2005). Sorting of vesicular monoamine transporter 2 to the regulated secretory pathway confers the somatodendritic exocytosis of monoamines. Neuron *48*, 619–633.

Liang, C.L., Nelson, O., Yazdani, U., Pasbakhsh, P., and German, D.C. (2004). Inverse relationship between the contents of neuromelanin pigment and the vesicular monoamine transporter-2: human midbrain dopamine neurons. J. Comp. Neurol. *473*, 97–106.

Lotharius, J., Barg, S., Wiekop, P., Lundberg, C., Raymon, H.K., and Brundin, P. (2002). Effect of mutant α-synuclein on dopamine homeostasis in a new human mesencephalic cell line. J. Biol. Chem. *277*, 38884–38894.

Martinez-Vicente, M., Talloczy, Z., Kaushik, S., Massey, A.C., Mazzulli, J., Mosharov, E.V., Hodara, R., Fredenburg, R., Wu, D.C., Follenzi, A., et al. (2008). Dopamine-modified α-synuclein blocks chaperone-mediated autophagy. J. Clin. Invest. *118*, 777–788.

Mena, M.A., Davila, V., and Sulzer, D. (1997). Neurotrophic effects of L-DOPA in postnatal midbrain dopamine neuron/cortical astrocyte cocultures. J. Neurochem. *69*, 1398–1408.

Moore, D.J., West, A.B., Dawson, V.L., and Dawson, T.M. (2005). Molecular pathophysiology of Parkinson's disease. Annu. Rev. Neurosci. *28*, 57–87.

Mosharov, E.V., Gong, L.W., Khanna, B., Sulzer, D., and Lindau, M. (2003). Intracellular patch electrochemistry: regulation of cytosolic catecholamines in chromaffin cells. J. Neurosci. *23*, 5835–5845.

Mosharov, E.V., Staal, R.G., Bove, J., Prou, D., Hananiya, A., Markov, D., Poulsen, N., Larsen, K.E., Moore, C.M., Troyer, M.D., et al. (2006). α-synuclein overexpression increases cytosolic catecholamine concentration. J. Neurosci. *26*, 9304–9311.

Moszczynska, A., Fitzmaurice, P., Ang, L., Kalasinsky, K.S., Schmunk, G.A., Peretti, F.J., Aiken, S.S., Wickham, D.J., and Kish, S.J. (2004). Why is parkinsonism not a feature of human methamphetamine users? Brain *127*, 363–370.

Nedergaard, S., Flatman, J.A., and Engberg, I. (1993). Nifedipine- and ω-conotoxin-sensitive Ca^{2+} conductances in guinea-pig substantia nigra pars compacta neurones. J. Physiol. *466*, 727–747.

Nicholson, C. (1999). Diffusion of ions and macromolecules in brain tissue. In Monitoring Molecules in Neuroscience, H. Rollema, E. Abercrombie, D. Sulzer, and J. Zackheim, eds. (Newark, NJ: Rutgers University Press), pp. 71–73.

Olanow, C.W., Agid, Y., Mizuno, Y., Albanese, A., Bonuccelli, U., Damier, P., De Yebenes, J., Gershanik, O., Guttman, M., Grandas, F., et al. (2004). Levodopa in the treatment of Parkinson's disease: current controversies. Mov. Disord. *19*, 997–1005.

Pardo, B., Mena, M.A., Casarejos, M.J., Paino, C.L., and De Yebenes, J.G. (1995). Toxic effects of L-DOPA on mesencephalic cell cultures: protection with antioxidants. Brain Res. *682*, 133–143.

Pothos, E.N., Davila, V., and Sulzer, D. (1998). Presynaptic recording of quanta from midbrain dopamine neurons and modulation of the quantal size. J. Neurosci. *18*, 4106–4118.

Pothos, E.N., Larsen, K.E., Krantz, D.E., Liu, Y., Haycock, J.W., Setlik, W., Gershon, M.D., Edwards, R.H., and Sulzer, D. (2000). Synaptic vesicle transporter expression regulates vesicle phenotype and quantal size. J. Neurosci. *20*, 7297–7306.

Rajadhyaksha, A.M., and Kosofsky, B.E. (2005). Psychostimulants, L-type calcium channels, kinases, and phosphatases. Neuroscientist *11*, 494–502.

Rajadhyaksha, A., Husson, I., Satpute, S.S., Kuppenbender, K.D., Ren, J.Q., Guerriero, R.M., Standaert, D.G., and Kosofsky, B.E. (2004). L-type Ca^{2+} channels mediate adaptation of extracellular signal-regulated kinase 1/2 phosphorylation in the ventral tegmental area after chronic amphetamine treatment. J. Neurosci. *24*, 7464–7476.

Rayport, S., Sulzer, D., Shi, W.X., Sawasdikosol, S., Monaco, J., Batson, D., and Rajendran, G. (1992). Identified postnatal mesolimbic dopamine neurons in culture: morphology and electrophysiology. J. Neurosci. *12*, 4264–4280.

Ricaurte, G.A., Guillery, R.W., Seiden, L.S., Schuster, C.R., and Moore, R.Y. (1982). Dopamine nerve terminal degeneration produced by high doses of methylamphetamine in the rat brain. Brain Res. *235*, 93–103.

Rice, M.E., Cragg, S.J., and Greenfield, S.A. (1997). Characteristics of electrically evoked somatodendritic dopamine release in substantia nigra and ventral tegmental area in vitro. J. Neurophysiol. *77*, 853–862.

Sampaio-Maia, B., Serrao, M.P., and Soares-da-Silva, P. (2001). Regulatory pathways and uptake of L-DOPA by capillary cerebral endothelial cells, astrocytes, and neuronal cells. Am. J. Physiol. Cell Physiol. *280*, C333–C342.

Sang, T.K., Chang, H.Y., Lawless, G.M., Ratnaparkhi, A., Mee, L., Ackerson, L.C., Maidment, N.T., Krantz, D.E., and Jackson, G.R. (2007). A *Drosophila* model of mutant human parkin-induced toxicity demonstrates selective loss of dopaminergic neurons and dependence on cellular dopamine. J. Neurosci. *27*, 981–992.

Sawamoto, K., Nakao, N., Kobayashi, K., Matsushita, N., Takahashi, H., Kakishita, K., Yamamoto, A., Yoshizaki, T., Terashima, T., Murakami, F., et al. (2001). Visualization, direct isolation, and transplantation of midbrain dopaminergic neurons. Proc. Natl. Acad. Sci. USA *98*, 6423–6428.

Striessnig, J., Koschak, A., Sinnegger-Brauns, M.J., Hetzenauer, A., Nguyen, N.K., Busquet, P., Pelster, G., and Singewald, N. (2006). Role of voltage-gated L-type Ca^{2+} channel isoforms for brain function. Biochem. Soc. Trans. *34*, 903–909.

Sulzer, D. (2007). Multiple hit hypotheses for dopamine neuron loss in Parkinson's disease. Trends Neurosci. *30*, 244–250.

Sulzer, D., and Pothos, E.N. (2000). Regulation of quantal size by presynaptic mechanisms. Rev. Neurosci. *11*, 159–212.

Sulzer, D., and Zecca, L. (2000). Intraneuronal dopamine-quinone synthesis: a review. Neurotox. Res. *1*, 181–195.

Sulzer, D., Bogulavsky, J., Larsen, K.E., Behr, G., Karatekin, E., Kleinman, M.H., Turro, N., Krantz, D., Edwards, R.H., Greene, L.A., and Zecca, L. (2000). Neuromelanin biosynthesis is driven by excess cytosolic catecholamines not accumulated by synaptic vesicles. Proc. Natl. Acad. Sci. USA *97*, 11869–11874.

Sulzer, D., Sonders, M.S., Poulsen, N.W., and Galli, A. (2005). Mechanisms of neurotransmitter release by amphetamines: a review. Prog. Neurobiol. *75*, 406–433.

Sulzer, D., Mosharov, E., Talloczy, Z., Zucca, F.A., Simon, J.D., and Zecca, L. (2008). Neuronal pigmented autophagic vacuoles: lipofuscin, neuromelanin, and ceroid as macroautophagic responses during aging and disease. J. Neurochem. *106*, 24–36.

Surmeier, D.J. (2007). Calcium, ageing, and neuronal vulnerability in Parkinson's disease. Lancet Neurol. *6*, 933–938.

Thompson, L., Barraud, P., Andersson, E., Kirik, D., and Bjorklund, A. (2005). Identification of dopaminergic neurons of nigral and ventral tegmental area subtypes in grafts of fetal ventral mesencephalon based on cell morphology, protein expression, and efferent projections. J. Neurosci. *25*, 6467–6477.

Tohgi, H., Abe, T., Yamazaki, K., Saheki, M., Takahashi, S., and Tsukamoto, Y. (1995). Effects of the catechol-O-methyltransferase inhibitor tolcapone in Parkinson's disease: correlations between concentrations of dopaminergic substances in the plasma and cerebrospinal fluid and clinical improvement. Neurosci. Lett. *192*, 165–168.

Tohgi, H., Abe, T., Saheki, M., Yamazaki, K., and Murata, T. (1997). Concentration of catecholamines and indoleamines in the cerebrospinal fluid of patients with vascular parkinsonism compared to Parkinson's disease patients. J. Neural Transm. *104*, 441–449.

Ved, R., Saha, S., Westlund, B., Perier, C., Burnam, L., Sluder, A., Hoener, M., Rodrigues, C.M., Alfonso, A., Steer, C., et al. (2005). Similar patterns of mitochondrial vulnerability and rescue induced by genetic modification of α-synuclein, parkin, and DJ-1 in *Caenorhabditis elegans*. J. Biol. Chem. *280*, 42655–42668.

Wightman, R.M., Jankowski, J.A., Kennedy, R.T., Kawagoe, K.T., Schroeder, T.J., Leszczyszyn, D.J., Near, J.A., Diliberto, E.J., Jr., and Viveros, O.H. (1991). Temporally resolved catecholamine spikes correspond to single vesicle release from individual chromaffin cells. Proc. Natl. Acad. Sci. USA *88*, 10754–10758.

Williams, J.T., North, R.A., Shefner, S.A., Nishi, S., and Egan, T.M. (1984). Membrane properties of rat locus coeruleus neurones. Neuroscience *13*, 137–156.

Young, E.A., Duchemin, A.M., Neff, N.H., and Hadjiconstantinou, M. (1998). Parallel modulation of striatal dopamine synthetic enzymes by second messenger pathways. Eur. J. Pharmacol. *357*, 15–23.

Zecca, L., Tampellini, D., Gerlach, M., Riederer, P., Fariello, R.G., and Sulzer, D. (2001). Substantia nigra neuromelanin: structure, synthesis, and molecular behaviour. Mol. Pathol. *54*, 414–418.